EVAPORATION: A TECHNIQUE FOR VISUALIZING MESH QUALITY

Lisa Durbeck

University of Utah, Salt Lake City, UT, U.S.A. ldurbeck@cs.utah.edu

ABSTRACT

The work described here addresses information generated during mesh preprocessing, specifically mesh quality indicators derived on a per-element basis. A technique is introduced for visualizing per-element quality indicators which allows the researcher to see the spatial distribution of the indicator across the entire mesh. The technique uses time as a display axis, creating a succession of images in which the mesh is gradually eroded down to its "worst" elements. The technique is described algorithmically here and is applied to an example. In addition to supplying the user with the locations of the worst mesh elements, the technique appears to provide its user with a good high-level understanding of the relationship between mesh geometry and quality. This may also prove to be a useful technique for observing successive refinements of a mesh.

Keywords: mesh generation, mesh refinement, mesh adaptation, preprocessing, mesh visualization, finite element mesh quality, unstructured tetrahedral meshes

1. INTRODUCTION

It is hard for users to investigate per-element information within a visualization of a finite element mesh. This is particularly true when the mesh is visually complex: unstructured, 3-dimensional, or contains many elements. During mesh quality analysis, the more elements one has to investigate, the harder the task of locating and fixing problems within the mesh. This paper introduces a technique for visualizing quantities defined over the set of mesh elements in a manner which simplifies the investigation. The technique is simple to implement, and the meaning of the resulting visualization is easy to interpret. The usefulness of this technique for visual mesh quality analysis is demonstrated by an example, application to a 16,000-element three-dimensional, unstructured, h-adapted, tetrahedral finite element mesh.

2. BACKGROUND

The history of the ongoing search for good metrics for guaging mesh quality is presented in [1]. Contributors to mesh quality are: the problem the researcher is trying to solve, the error from the equations used, the norm used, and the mesh geometry [1]. These contributors can be distilled into one or more quality indicators. Some examples are error estimates based on mesh elements' shapes, sizes, and the positions of element vertices. The primary goals during mesh quality analysis are not only locating the worst mesh elements but also determining the causes for bad elements. This requires first finding each problem area, then isolating it for further study.

A typical mesh contains on order of 100,000 elements. It is hard to visualize them all in a full 3D mesh display, particularly in regions densely packed with small elements, and it is difficult to comprehend fully the myriad of element shapes and sizes. Views of the full mesh, showing the outline of the elements in wire-frame mode or showing each element as a colored solid, are not useful for the investigation of individual mesh elements -- or of quantities defined over the set of elements – because the granularity is wrong. It's like requiring the user to find a needle in a haystack: the sheer number of elements and the way they are packed makes investigation of a display containing all of them too time-consuming to be viable.

Techniques have been developed for mesh analysis and manipulation of unstructured meshes. Some display the mesh

visually, some display a tree version of node connectivity, others provide file-based or batch-mode interaction [2]. One particular mesh analysis tool is MeshView [3]. The technique described here is an extension, application, and automation of a feature of MeshView, namely user-controlled views of subsets of the mesh.

MeshView provided a histogram-based user control identical to the one shown in the methods section. The user could specify a subrange of the mesh for display by interacting with the slider bars on the histogram. After specifying a subrange, the user could indicate that it should be drawn. However, there is an advantage in being able to being able to easily and rapidly see successive frames corresponding to the user's line of inquiry. Being able to hit a single button and then just watch as the filtering "happens" in a timely fashion has clear advantages over having to perform complex interactions to bring up each successive frame.

This improved display technique was applied to the problem of visually analyzing the spatial distribution of error in a mesh. An increasingly narrow high-pass filter was applied to the data. The user is able to watch the filtering and relatively easily compare successive frames. The filter was incorporated into the user interface so that the user could invoke it with one click and watch the results. This work is part of a larger body of research toward designing an interactive user interface for mesh quality analysis [4].

3. METHODS

The Evaporation visualization technique was applied to a given mesh and a set of error indicators defined for the set of mesh elements from a shock-dominated problem [5]. The shock wave mesh and indicators were created by the TETRAD mesh adaptation software [6], which produces unstructured tetrahedral meshes. This section uses the shock wave mesh and error indicators to describe the technique; however, the same technique may be used for a wide variety of meshes and quality indicators.

The technique was implemented for unstructured tetrahedral meshes within SCIRun, a programming environment for scientific computing [7][8]. SCIRun provided much of the infrastructure necessary for manipulating the mesh and creating graphical output.

For this technique, the tetrahedra are assigned colors based on a mapping from error indicator values to a set of color bins. All tetrahedra are displayed as shaded solids, as shown in Figure 1. Color provides information about the level of error, and facet shading provides information about element shape and orientation.
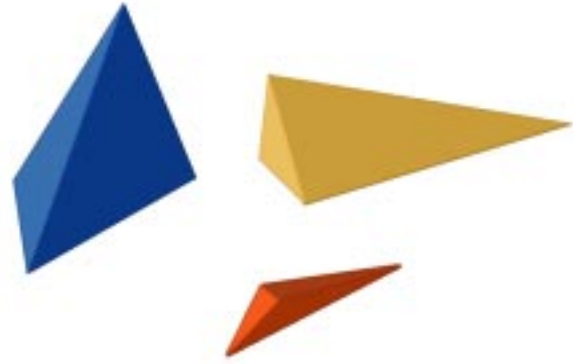

Figure 1. For this technique, individual tetrahedra are drawn as shaded solids

The distribution of error indicators for the given mesh is shown in Figure 2. The lowest bin, which contains approximately 15,500 elements, has been dropped off the figure so that the remaining bins are visible.
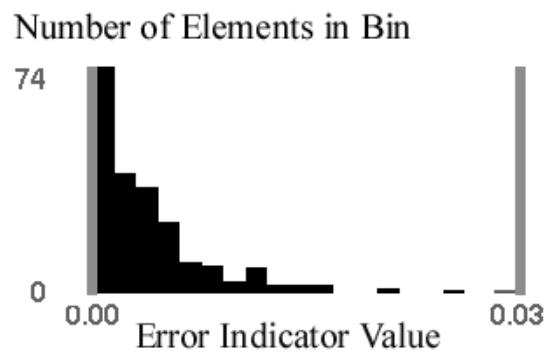

Figure 2. Histogram showing the distribution of error indicator values across the mesh. Black vertical bars are bins; grey vertical bars indicate the range to be displayed. Error indicator values are displayed along the x axis; the y-axis indicates the number of elements which fall into each bin. The axes have been truncated for better readability.

A high-pass filter is applied to the data repeatedly and the results are displayed at each pass.The visualization proceeds as follows: the mesh is visualized as a series of frames like a movie. At first, all mesh elements are drawn. At each pass, the "best" of the remaining elements are "evaporated," leaving the worst, which are then subjected again to evaporation, leaving successively smaller sets of bad elements. Over the course of the visualization, the mesh is eroded in steps down to just the worst element. The histogram in Figure 2 is useful for describing the visualization technique. The lefthand range indicator is gradually moved to the right over time, restricting the display to a smaller and smaller subset of the mesh elements. This progression is illustrated in Figure 3.

These figures describe the technique, not the resulting images. In the next section, the resulting time-series visualizations of the shock wave mesh are shown.

The technique was also applied to an air pollution model with complex interactions between multiple pollutants [9]. Evaporation visualizations for two different error indicators based on two different chemicals are presented in the Results section. Error indicators are from a simple first-order calculation based on gradients [4].

Figure 3. This series shows a simplified version of the histogram in order to demonstrate how the visualization technique proceeds. It begins with all mesh elements, as displayed in Figure 2. The lefthand range bar is moved right in a series of steps. Only those mesh elements within the two range indicators are drawn.

4. RESULTS

This technique was applied to the shock wave mesh to display the spatial distribution of error indicator values across the mesh. The resulting time series is shown as a film strip in Figure 4; in practice, the film strip was run like a movie projector: the images were shown in place to give the effect of a moving image. A movie version of the same figure is provided at http://www.cs.utah.edu/~ldurbeck/imr99. An inverse rainbow color map was used to color the mesh elements. The best elements are blue, and the worst are red.

Several features of the spatial distribution of error indicators are visible from comparisons of the frames within Figure 4. With the given color map, as time proceeds, the visualization drops off first the blue, then the green, then the orange elements, leaving the lone red element in the final image. The large jump from the first to the second frames indicates that most of the mesh elements have extremely low error indicator values. Multiple frames show that the worst mesh elements lie within a roughly planar section of the mesh. Of those elements, the color distribution indicates that the remaining elements in the final two frames are outliers; this is indicated by the fact that they range from middle green to red, taking up over half the overall color range, and yet their numbers are few.
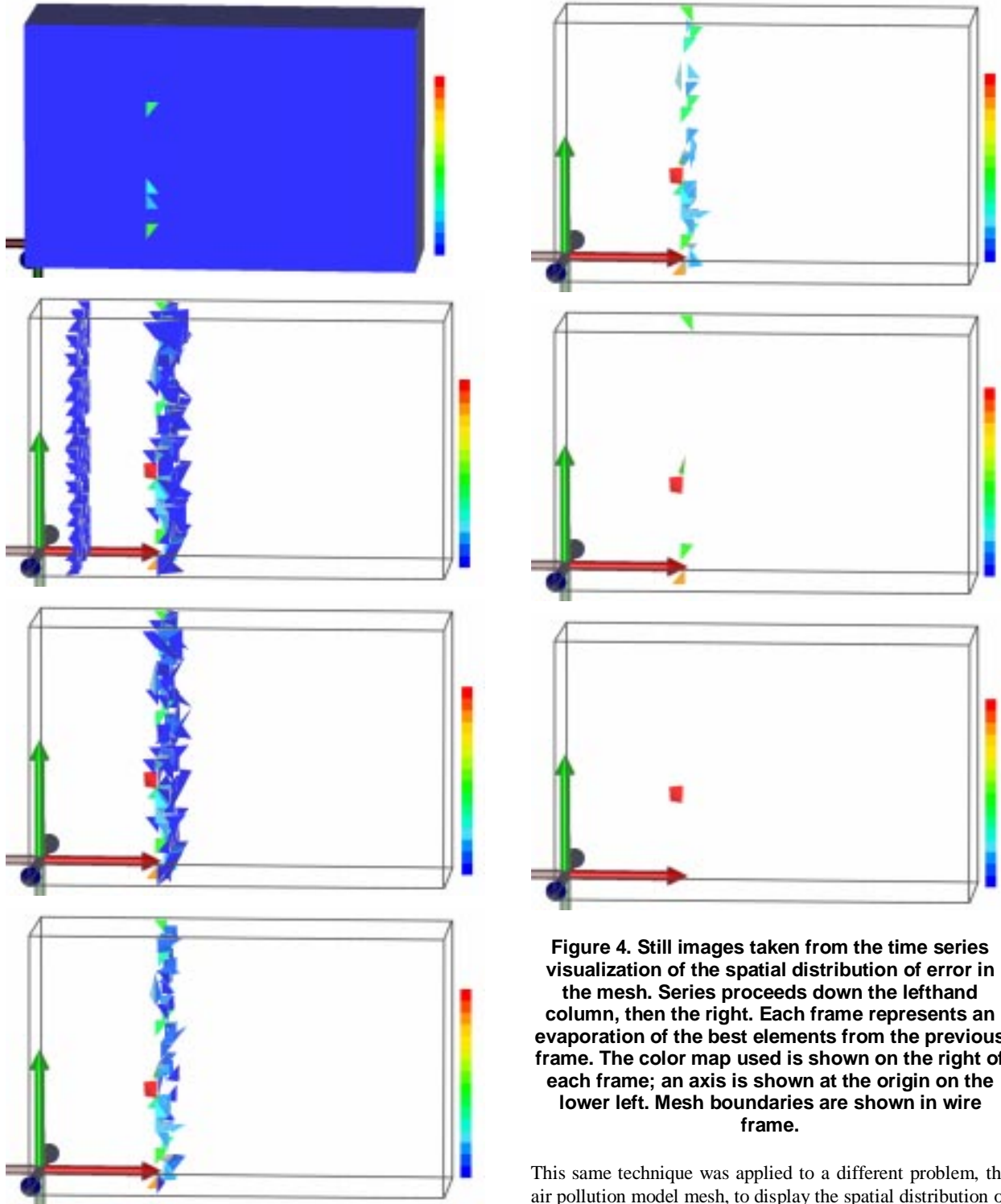
Figure 4. Still images taken from the time series visualization of the spatial distribution of error in the mesh. Series proceeds down the lefthand column, then the right. Each frame represents an evaporation of the best elements from the previous frame. The color map used is shown on the right of each frame; an axis is shown at the origin on the lower left. Mesh boundaries are shown in wire frame.

This same technique was applied to a different problem, the air pollution model mesh, to display the spatial distribution of error indicator values across the mesh. Still images from the series are shown in Figure 5 and Figure 6. Different error indicators were used to generate the two figures.

Comparison of the two figures is revealing. The distributions both the error values and locations are in stark contrast, but also show some commonalities. Error indicator 1 in Figure 5 flags a small number of mesh elements as being problematic

(i.e. 14 green to red elements) spatially limited to one small region of the mesh. Of those, two are markedly worse than the rest, the single red and the single yellow-green element.

Error indicator 2 in Figure 6 flags a large number of elements as being poor quality; their colors and time-to-disappear indicate a fairly normal distribution of error. The "bad" elements range across the entire mesh, with the worst roughly aligned along the upper half of the mesh. The set of red elements, i.e., the worst elements in the mesh, lie clustered around approximately the same region as flagged by error indicator 1.

Taken together, these two series provide evidence that this evaporation technique is useful for visual comparison of two different error metrics.
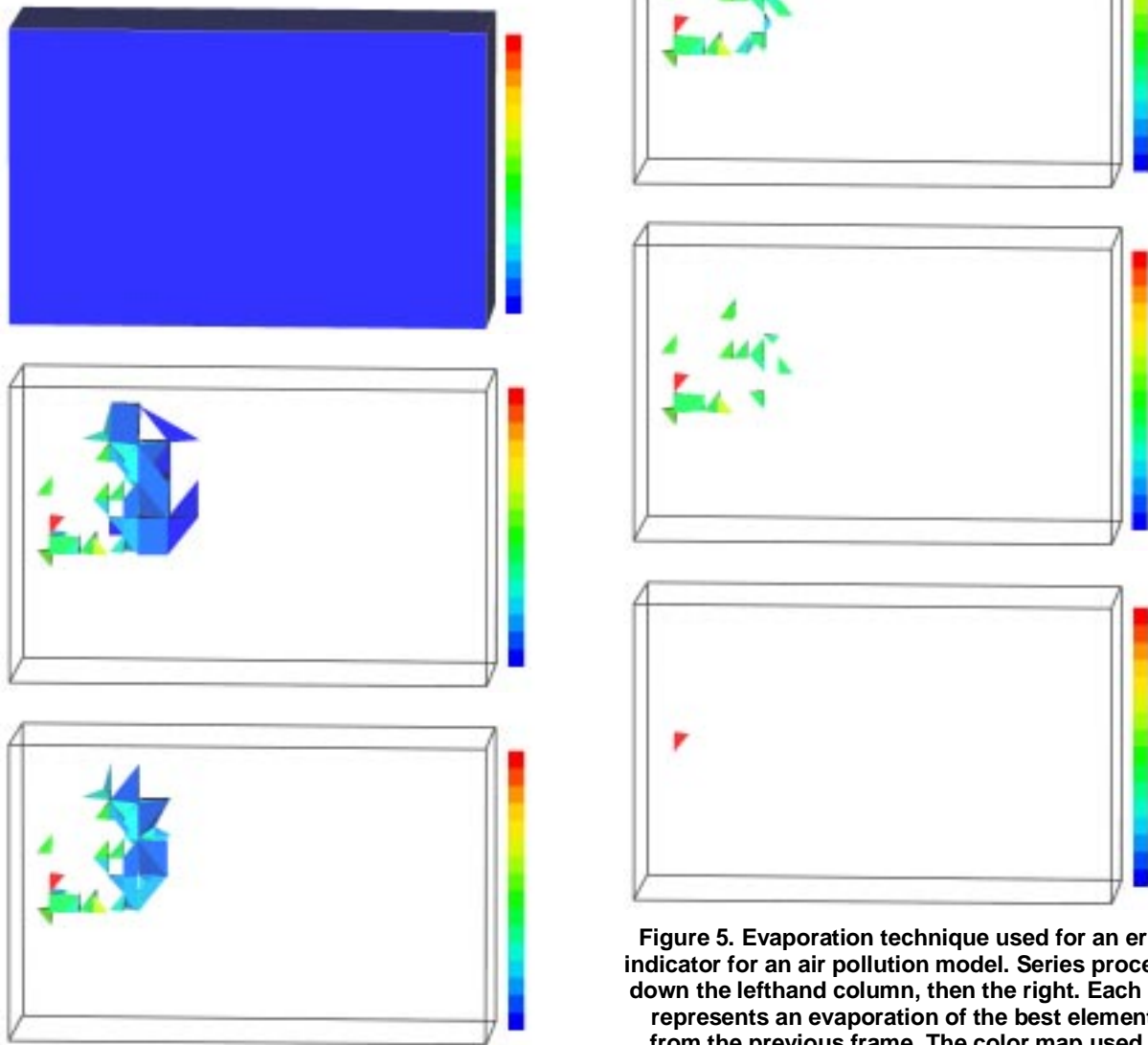

Figure 5. Evaporation technique used for an error indicator for an air pollution model. Series proceeds down the lefthand column, then the right. Each still represents an evaporation of the best elements from the previous frame. The color map used is shown on the right of each frame. The mesh boundaries are drawn in wire frame.
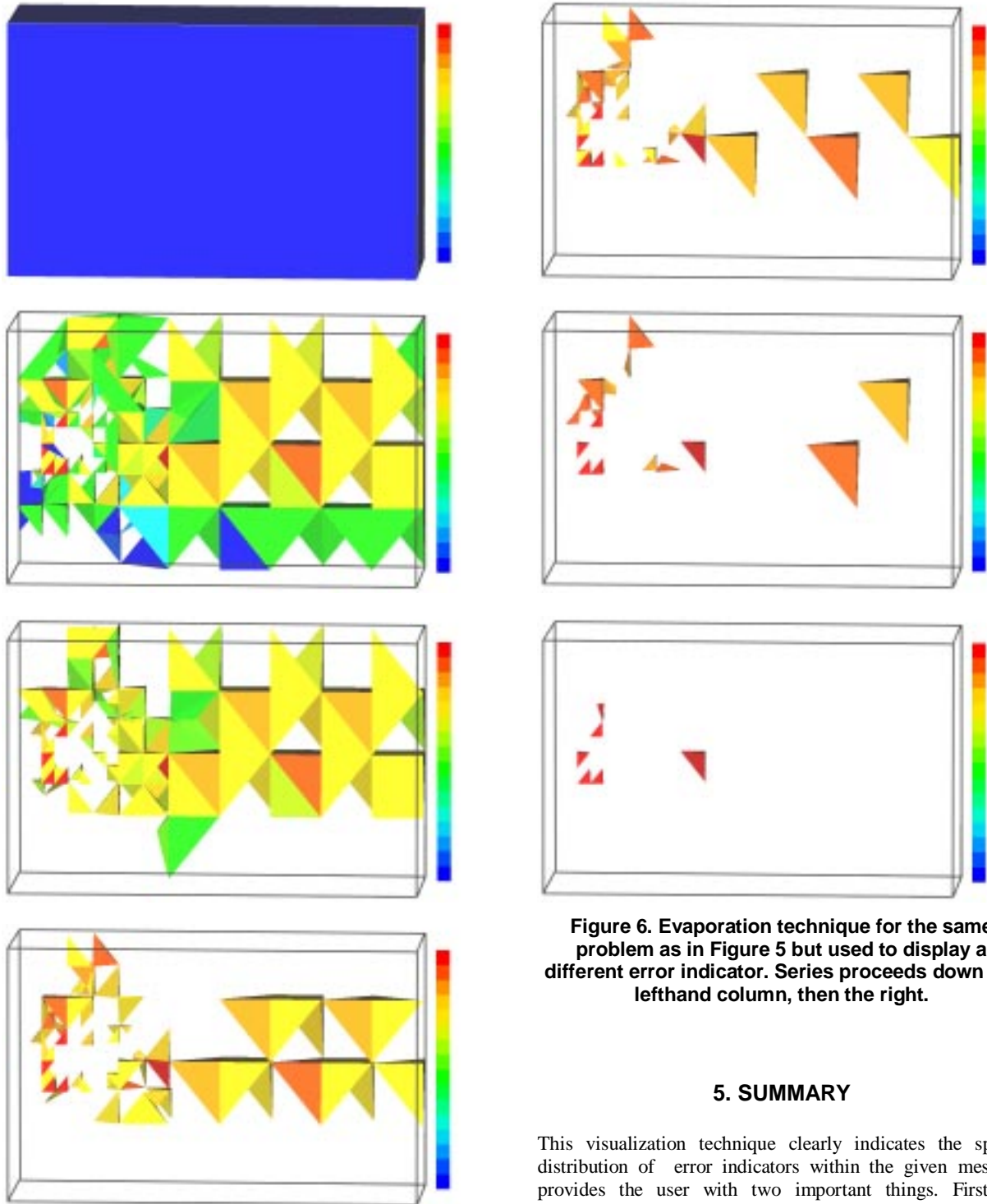
Figure 6. Evaporation technique for the same problem as in Figure 5 but used to display a different error indicator. Series proceeds down the lefthand column, then the right.

5. SUMMARY

This visualization technique clearly indicates the spatial distribution of error indicators within the given mesh. It provides the user with two important things. First, by reducing the mesh down to its worst elements, it identifies and isolates the trouble spots for the user. Second, by displaying the evaporation as a moving image, the pattern of error for the mesh as a whole is made evident to the user. This provides the user with high level information needed to deduce the potential reasons for poor quality.

The results presented here provide visual evidence that this may be a promising visualization technique for investigating per-element mesh quality indicators within the geometrical

context of the mesh. In the case of the air pollution model, using this technique we were able to quickly identify the different refinement strategies indicated by two potential refinement criteria. Not only were we able to see which elements they flagged as being most in need of refinement, but we were able to see that they flagged markedly different percentages of the mesh as "bad," and different but partially overlapping regions as bad.

The evaporation technique it provides interesting and useful visual information about the distribution of error in the mesh. Its implementation is straightforward, and the general technique can likely be profitably applied to other per-element quantities.

6. FUTURE WORK

This technique could be extended in several directions. The mapping from the quality indicator to time could be further investigated: user-controlled transfer functions and other nonlinear mappings may make important information about the mesh quality available to the user. Use of this technique for a variety of mesh and quality indicators should indicate a set of useful mappings. Since it works at a fairly high, "trend" level, the technique may also be extendable to multiple independent, or semi-independent quality metrics displayed at once in the same, or separate, windows. Modifications could also be made to make this technique useful for information captured on a per-vertex basis as well, perhaps by using point clouds or shading of the element faces based on combinations of their vertex values.

Work with this technique continues. The usefulness of this technique for visualizing intermediate results in a steering environment, for use with a mesh refinement package, is currently under investigation.

ACKNOWLEDGEMENTS

REFERENCES

[1]   Berzins, Martin. "Mesh Quality: A Function of Geometry, Error Estimates or Both?" *Mini-Tutorial, 7th International Meshing Roundtable, 16-18 October 1998.*

[2]   Carey, Graham F. *Computational Grids: Generation, Adaptation, and Solution strategies*. Computational and Physical Processes in Mechanics and Thermal Sciences 4. Washington, D.C: Taylor and Francis, 1997.

[3]   Gitlin, C.S. and C.R. Johnson. "MeshView: A tool for exploring 3D unstructured tetrahedral meshes." *Proceedings of the 5th International Meshing Roundtable*, 1996: 333-345.

[4]   Durbeck, Lisa J. K. "Contrast Displays: An Interactive Haptic and Visual Interface Designed for Mesh Quality Analysis." Thesis, University of Utah, 1999.

[5]   Speares, William, and Martin Berzins. "A 3D Unstructured Mesh Adaptation Algorithm for Time-Dependent Shock-dominated Problems." *International Journal for Numerical Methods in Fluids* 25 1997: 81-104.

[6]   Speares, William. *TETRAD Software User Guide V103* technical document, School of Computer Studies, University of Leeds, England, November 1995.

[7]   Parker, S. G., D. M. Weinstein, and C. R. Johnson. "The SCIRun Computational Steering Software System." *Modern Software Tools in Scientific Computing*, E. Arge, A.M. Bruaset, and H.P. Langtangen, eds. Birkhauser Press, 1997: 1-44.

[8]   Parker, S.G. and C. R. Johnson. "SCIRun: A Scientific Programming Environment for Computations Steering." *Proceedings of the 1995 ACM/IEEE Supercomputing Conference. San Diego, 3-8 Dec. 1995.* <http://www.supercomp.org/sc95/proceedings/SC95MAIN.HTM>.

[9]   Johnson, C.R., M. Berzins, L. Zhukov, and R. Coffey. "SCIRun: Applications to Atmospheric Diffusion Using Unstructured Meshes*." Numerical Methods for Fluid Dynamics VI*. Ed. M. J. Baines. Oxford: Oxford University Press, 1998. 111-122.